Communications Research Centre

THE DEPENDENCE OF HF DIRECTION FINDING ACCURACY ON APERTURE SIZE

by

L.E. Montbriand

This work was sponsored by the Department of National Defence, Research and Development Branch under Project No. 32G01.

DEPARTMENT OF COMMUNICATIONS
MINISTÈRE DES COMMUNICATIONS

CRC REPORT NO. 1343

CANADA

OTTAWA, JUNE 1981

COMMUNICATIONS RESEARCH CENTRE

DEPARTMENT OF COMMUNICATIONS
CANADA

THE DEPENDENCE OF HF DIRECTION FINDING ACCURACY ON APERTURE SIZE

by

L.E. Montbriand

(Radar and Communications Technology Branch)

CRC REPORT NO. 1343

June 1981

OTTAWA

This work was sponsored by the Department of National Defence, Research and Development Branch under Project No. 32G01.

TABLE OF CONTENTS

THE DEPENDENCE OF HF DIRECTION FINDING ACCURACY ON APERTURE SIZE

by

L.E. Montbriand

ABSTRACT

A 1943 m by 236 m crossed linear array located at Ottawa was used to investigate the relationships between direction finding accuracy, wavefront planarity, and aperture size. Two tests were carried out: Test A: transmissions from Sept Iles, Quebec to Ottawa (a 911 km path), and Test B: from San Antonio, Texas to Ottawa (2654 km path). An FMCW sounding technique was employed which made it possible to resolve modes differing in time of arrival by as little as 20 μs. Transmissions during Test A were via E, E_S, 2E, $2E_S$, F1, F2 and 2F1 modes and during Test B via $2E_S$, F1, F2 and 2F2 modes.

The data for the long arm of the array were processed in sub-sets so as to provide results for 9 different aperture sizes. Three basic comparisons were made. The first concerned the relationship of apparent wavefront planarity to aperture size, where the measure of the planarity (RMSD) was the RMS of phase deviations from a straight line fit of phases along the array. The second comparison concerned the relationship of the standard deviation of bearing to aperture size, and the third, the relationship of bearing error to wavefront planarity. For both tests the standard deviation in the bearing decreases with increasing aperture size. For Test A the standard deviation at 100 m and 1000 m respectively is near 1.0 and 0.4 degrees for the E modes, 2.5 and 1.5 degrees for the various F1 modes and 2.5 and 2.0 degrees for the F2 modes. For Test B the standard deviation at 100 m and 1000 m respectively is near 0.2 and 0.2 degrees for the F1 mode, 0.8 and 0.5 degrees for the F2 low angle mode, 1.5 and 1.3 degrees for the F2 high angle mode and 1.0 and 0.5 degrees for the $2E_S$ mode. The RMS error in the mean bearing was found to be not critically dependent on the choice of the RMSD threshold one uses for accepting or rejecting data. Interpretation of these results and other implications in direction finding design are discussed.

1. INTRODUCTION

The dependence on aperture size of the accuracy with which the location of an unknown transmitter can be determined is of prime importance in radio direction finding (DF). Rice (1975) examined this problem using a swept frequency continuous wave (SFCW) signal transmitted from Sept Iles and received by the sampled aperture receiving array (SARA) at Ottawa. Results were presented for four aperture sizes (the largest 1181 m) for three ionospheric modes and for 40 hours of operation. This report presents more extensive results from a similar experiment conducted over the same path for a four day period and over a path three times as long for a three day period. Details of these tests, including path lengths and frequencies used are given in Table 1. Results for nine aperture sizes (the largest 1943 m) and for a variety of propagation modes are presented.

TABLE 1

Details of Test

	Dates of Test	Transmitter Location	Path Length	Frequencies Used
Test A	June 20 – 23, 1977	Sept Iles 50°12'N, 66°09'W	911 km	5.2 to 7.7 MHz
Test B	Nov. 20 – 25, 1977	San Antonio 29°27'N, 98°37'W	2654 km	7.6 to 23.4 MHz
		Receiver Location Ottawa 45°14'N, 75°51'W		

2. EXPERIMENTAL TECHNIQUE

The experimental arrangement for the measurements reported herein is similar to that described in Rice (1973) and Rice and Winacott (1977). A SFCW signal was transmitted from Sept Iles, Quebec, Canada for what is referred to as the medium path or Test A, and from San Antonio, Texas for the long path or Test B. For both tests a 50 kHz sweep was used and the transmitted signal was received at the Ottawa SARA site by a 62 element 1943 m by 236 m crossed linear array. Details are given in Table 1. This is the same array described in detail by Rice and Winacott (1977) except that four additional elements had been added to the original 1181 m arm in the north west direction at locations 1332 m, 1561 m, 1751 m and 1943 m from the south end. For both tests, the transmission was along the bore sight (perpendicular to) of long arm of the receiving array.

Data processing was carried out in such a way as to independently study nine aperture sizes on the long arm and three aperture sizes on the short arm. In addition, an alternate 1181 m aperture was included to establish, as it did, that effects arising from the municipal roadway and the power line crossing the array between the 1332 m and the 1561 m elements were unimportant, and that the reduction in signal-to-noise ratio resulting from the extra long cables to the four new elements was minor.

3. DATA REDUCTION

The data collection and processing techniques during the test were similar to those used by Rice (1975) but incorporated the amplitude to gain calibration as outlined by Burke (1978). The recorded data were processed in two stages. In the first stage, corrections for equipment parameters were made. These include removal of the characteristic phase of the individual receivers, and phase corrections for differences in cable lengths (Rice and Winacott, 1977). During this stage of processing, the data were also processed for range. The resulting output magnetic tape thus contained data presented in time-delay (range) vs receiver-number co-ordinates with each data point being a complex-number representation of signal amplitude and phase.

In the second stage of processing, calculations were carried out on ranges with significant signal strength, to yield azimuth, elevation and a measure of wavefront planarity at one minute intervals. The measure of wavefront planarity that was used was a weighted RMS deviation from a linear fit to the phases over the aperture. Since the antenna spacings were not uniform, but were concentrated near the centre of the array (cf. Rice and Winacott, 1977), the phase deviation at each element was weighted by the mean distance to its nearest neighbours divided by the average of all antenna spacings. This was an attempt to approximate the result that would be obtained if the array had uniform spacing. The RMS of such weighted phase deviations are referred to as RMSD in this report. In Table 2 are listed the various apertures, their weighted size and the number of receivers in that aperture. A minimum array spacing used in the experiment was 15.24 m, but a 22.86 m spacing at the centre of the array when used in conjunction with neighbouring antennas in a phase resolving algorithm provided a single effective spacing of 7.62 m corresponding to one-half wavelength at 19.685 MHz. Only in Test B were measurements made above this frequency. Signals for this test were accepted only if they appeared to arrive within ±90 degrees of the great circle direction. It is believed that a small number of cases for which there was still a directional ambiguity were incorporated into the results. In both tests it was assumed that 2π ambituities in the phase measurements from the more widely-spaced elements in the long array could be properly resolved by extrapolating the phase slope obtained from the close-spaced elements.

The next stage of processing involved relating the signals at various ranges with specific ionospheric modes of propagation. Modes were identified by comparision of the data in a range vs time display, together with the azimuth and elevation measurements, to the oblique ionograms which were made at 20 minute intervals during the course of the experiments. Those modes which were clearly separated in range and for which there was a statistically significant occurrence are listed for Test A in Table 3 and for Test B in Table 4. For Test A the frequency change was small and a frequency breakdown of the data did not change the results. As a consequence no such breakdown is presented. For Test B the range of frequencies was very large and such a breakdown was needed. Note that modes are sorted according to low and high angles, o and x components and night and day as well as ionospheric layer. For certain results such a breakdown into modes was found to be unnecessary and modes were combined. These are indicated in the text where this applies. For Test A the E_s mode has been broken down into three categories, and, as indicated elsewhere, each is different. Signals on the E_s-S-N mode arrived as much as 8 degrees south of the great circle direction.

TABLE 2

Details of Aperture

Long Arm

Aperture Size (m)		
Actual	**Weighted**	**No. of Receivers**
84	99	6
145	160	10
267	305	18
419	457	22
572	610	26
800	838	34
1181	1276	42
1181*	1295*	16
1562	1676	44
1943	2057	46

Short Arm

84	99	6
145	160	10
236	251	16

* *Alternate aperture*

TABLE 3

Modes Over Sept Iles to Ottawa Path (Test A)

Mode	Occurrences
E,L	1820
E,H	148
E_s-1-N (E_s present, no $2E_s$ identifiable; at night)	131
E_s-2-N (E_s with $2E_s$ also present; at night)	111
E_s-S-N (E_s from side direction; at night)	21*
2E (2 hop E)	303
$2E_s$	175
$2E_s$-N	130
F1(o,x),L (F1(o),L and F1(x),L; x and o not resolved)	436
F1(o),H	1072
F1(x),H	902
2F1(o),L	145
2F1(o),H	129
2F1(o),near MOF (near maximum observed frequency)	190
F2(o),L	654
F2(x),L	924
F2(o,x),L-N (F2(o),L and F2(x),L; x and o not resolved; at night)	204
F2(o),H	734
F2(o),H-N	154
F2(x),H	690
F2(x),near MOF	94

L – low angle

H – high angle

N – at night

**A unique result at 7.675 MHz on day 173 20:23 – 20:55 EST*

TABLE 4

Modes Over San Antonio to Ottawa Path (Test B)

Mode	Frequency	Occurrence
F1(o,x),L F1(o),L and F1(x), L; x and o not resolved	15.	36
$2E_S$-N	9.3	56
F2(o,x),L-N F2(o),L and F2(x),L; x and o not resolved	7.65	152
F2(o,x),L-N F2(o),L and F2(x),L; x and o not resolved	10.	480
F2(o,x),L-N F2(o),L and F2(x),L; x and o not resolved	15.	80
F2(o,x),L F2(o),L and F2(x),L; x and o not resolved	15.	225
F2(o,x),L F2(o),L and F2(x),L; x and o not resolved	21.	407
F2(o,x),L 2F(o),L and F2(x),L; x and o not resolved	23.4	91
F2(o),H-N	7.65	91
F2(x),H-N	7.65	89
F2(o),H-N	10.	108
F2(x),H-N	10.	111
F2(o,x),H-N F2(o),H and F2(x),H; x and o not resolved	10.	167
F2(o,x),H-N F2(o),H and F2(x),H; x and o not resolved	15.	33
F2(o,x),H F2(o),H and F2(x),H; x and o not resolved	21.	361
F2(o,x),H F2(o),H and F2(x),H; x and o not resolved	234	86
F2 near MOF-N	10.	93
F2 near MOF-N	234	53
2F2(o,x),L-N 2F2(o),H and 2F2(x),H; x and o not resolved	7.65	32
2F2(o,x),L 2F2(o),H and 2F2(x),H; x and o not resolved	15	371
2F2(o,x),H 2F2(o),H and 2F2(x),H; x and o not resolved	15.	64
2F2 near MOF-N 2F2(o),H and 2F2(x),H; x and o not resolved	10.	31
2F2 near MOF 2F2(o),H and 2F2(x),N; x and o not resolved	15.	53

L — low angle

H — high angle

N — at night

3.1 RESIDUAL ERRORS OF RECEIVER PHASES

The smallest values of RMSD over the 1943 m aperture for the two tests conducted were between 4 and 6 degrees. These values occur regularly for signals transmitted over the Sept Iles to Ottawa path for the low angle E mode and over the San Antonio to Ottawa path for F1 and F2 modes. As indicated by Montbriand, this apparent lower limit to the RMSD is due to residual phase errors in the various receiving channels. These errors remain after calibration of the receivers themselves and are attributable to errors in matching the antenna elements and cable system, to secondary reflections from nearby re-radiators, and to antenna mutual coupling effects. Some of this error is sufficiently systematic that it can be empirically determined from the data; in this report such errors are called residual phase errors of the receiver phases. They can be determined, for each receiver channel, from a large number of occurrences of phase fronts for which the RMSD is near the lower limit. The component of the RMSD due to these errors is actually a summation of the (weighted) contributions of those channels which are in the particular aperture. For Test A, based on five sets of residual phase errors for the low angle E mode and one set for the low angle F2(o) mode, a mean component of the residual errors was evaluated for each aperture. For Test B residual phase errors were obtained for all modes and frequencies. It is these values that were used where indicated. They are incorporated by first calculating for each receiver the phase of the received signal and then removing the residual phase error. The main effect that this produces is a substantial decrease in the RMSD value where the value is low ($<10°$).

3.2 RMSD VERSUS APERTURE

The RMSD can be used as a measure of wavefront planarity. The variation of this parameter with aperture is useful in understanding the effect that multipath and multimode interference have on the wavefront measurements. One approach which illustrates this variation is to plot the median RMSD against aperture for each of the modes and frequencies listed in Tables 3 and 4. This approach was not adopted because these results varied slightly with frequency, and because results for one mode for one time interval differed only slightly from those for the same mode or another mode but for another time interval. The approach adopted was to use results from all modes and all frequencies for each test to prepare a series of curves which would represent levels of wavefront non-planarity on an RMSD vs aperture plot. The advantage of this approach is that the RMSD vs aperture presentation for each test becomes far more compact than a series of graphs for each mode, and it allows for the great variability of ionospheric conditions from one test period to another and for the results of all modes to be presented on the same graph. Results representing different time intervals and the different modes were first used to plot, for each aperture, the median RMSD, with the component due to the residual phase errors removed, against that of a reference aperture (that for 1181 m was used). Plots for the 572 m and 1943 m apertures are presented in Figure 1 for Test A and in Figure 2 for Test B. A smooth line is drawn through the points in Figure 1 and a best fit straight line is drawn in Figure 2. The presentation of RMSD vs linear aperture accentuates the curve behaviour at short apertures; that of RMSD vs log aperture (not shown) accentuates the curve behaviour at long apertures. Similar curves can be obtained for other modes, and all of the curves can be

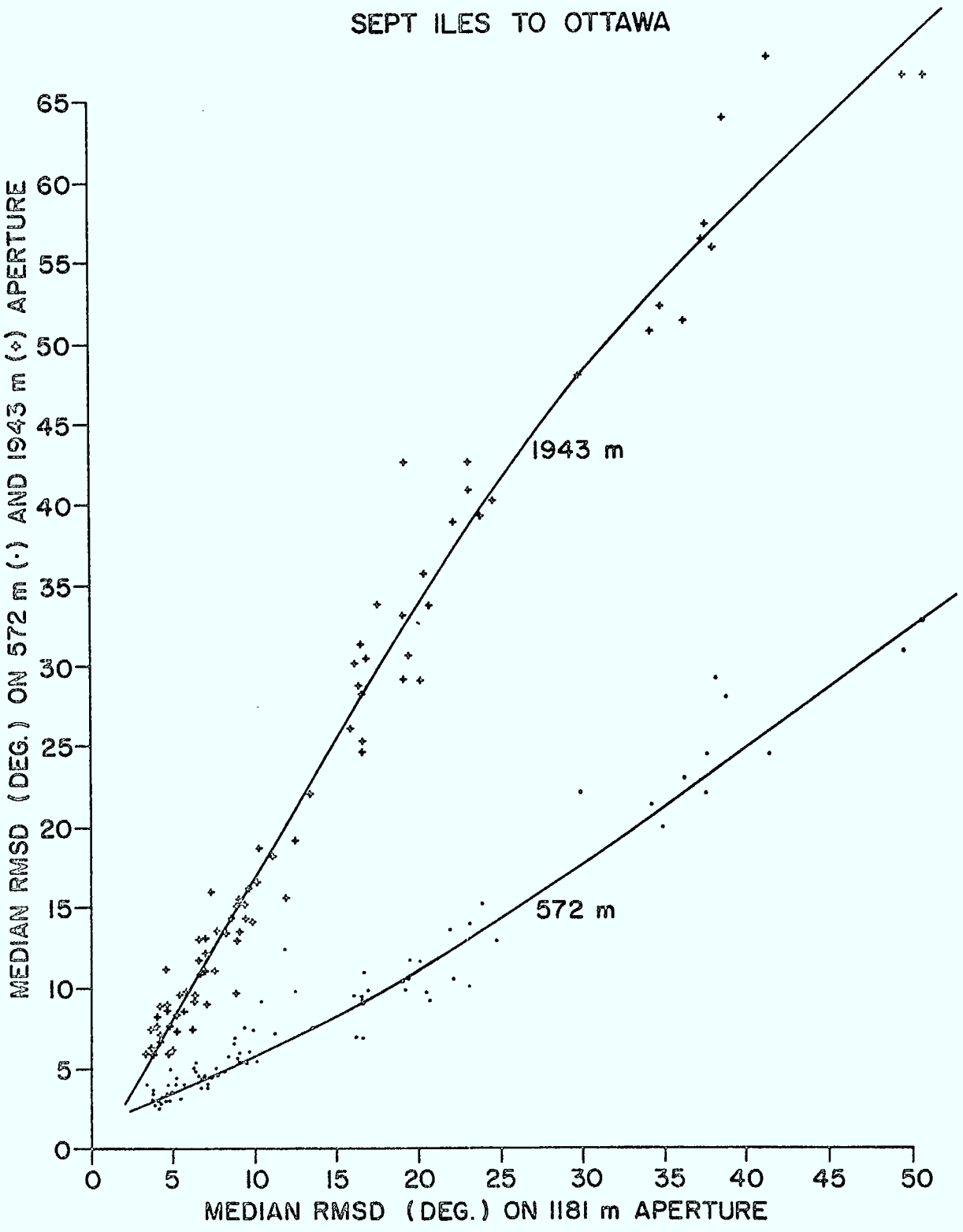

Figure 1. Median RMSD in degrees (with components due to residual phase errors removed) for all modes for the June 1977 Sept Iles to Ottawa Tests (Test A)

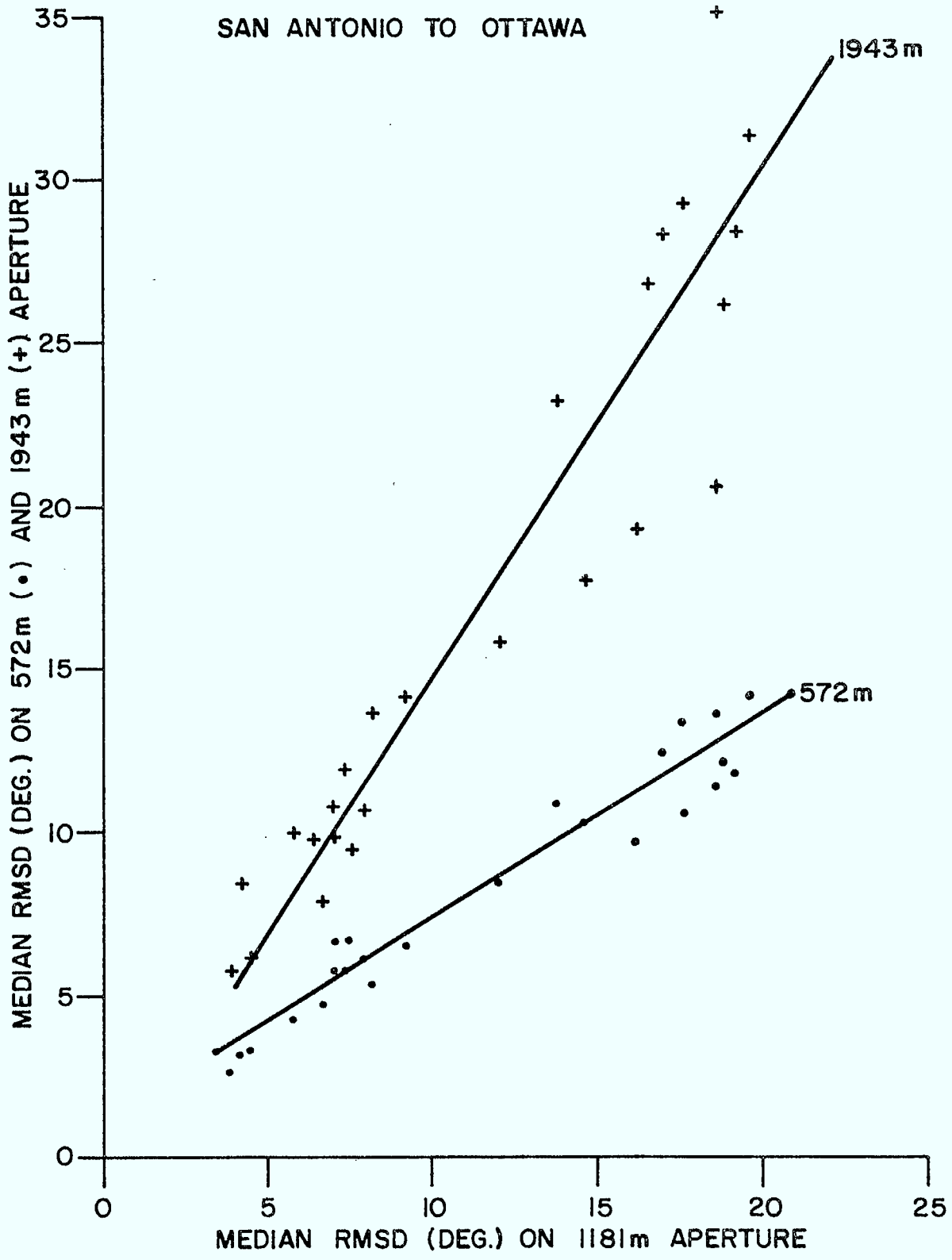

Figure 2. Median RMSD in degrees (with component due to residual phase errors removed) for all modes for the November 1977 San Antonio to Ottawa tests (Test B)

plotted on the same graph. An ordered representation of such a plot can be obtained by identifying each curve by the RMSD for an arbitrarily chosen aperture, 1181 m in our case, and interpolating the data to obtain curves for integral steps of RMSD at the 1181 m aperture. Such curves form the basis of Figures 3 and 4, where the curves can be interpreted to represent wavefronts of a given "roughness" or "non-planarity" (defined by the RMSD for an 1181 m aperture). These curves can be used to predict for an applicable test path the RMSD for any aperture knowing the RMSD for any other aperture, something previously not easily obtained.

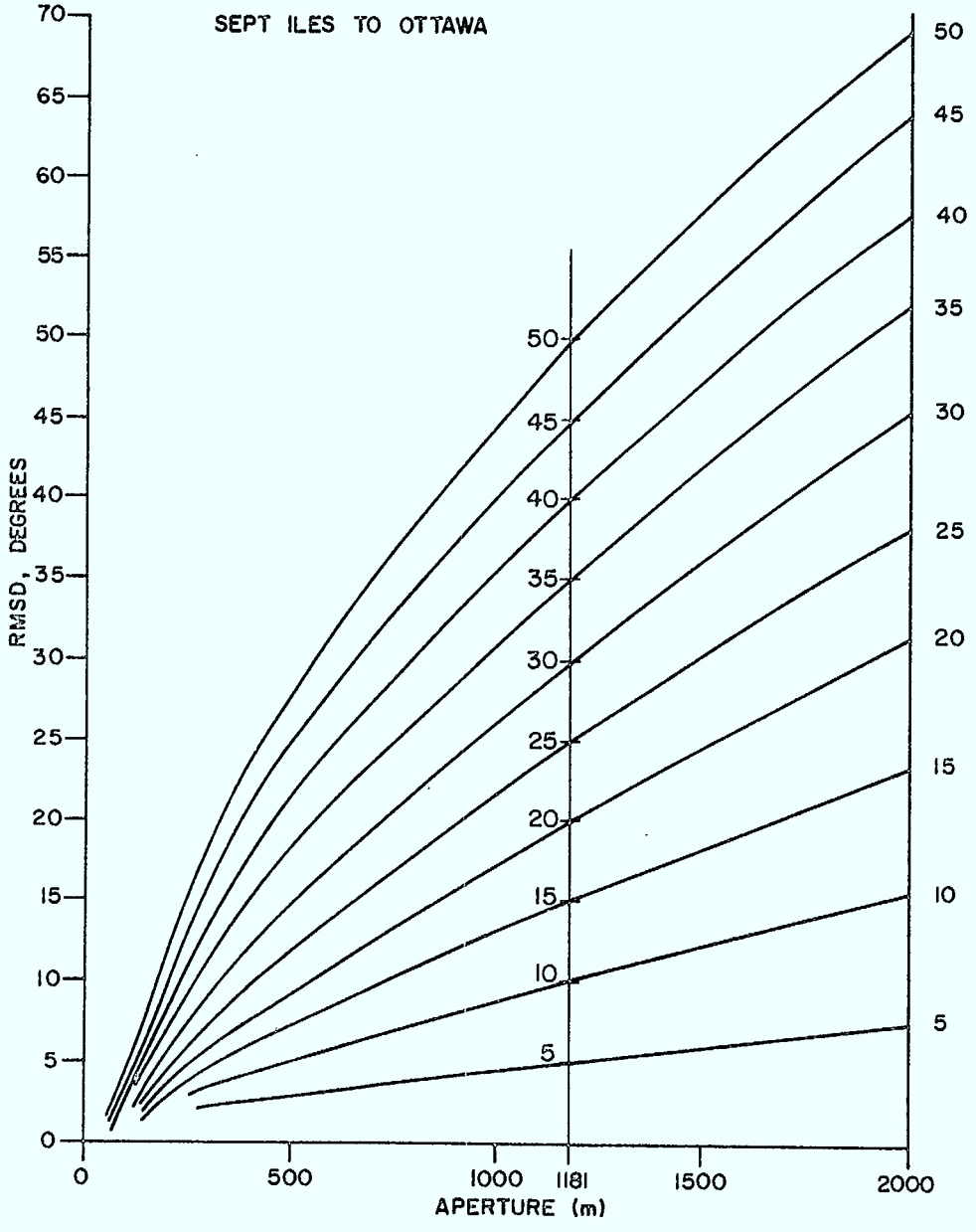

Figure 3. RMSD (with component due to residual phase errors removed) vs aperture for Test A. Curves are identified by the RMSD value at the vertical line at 1181 m.

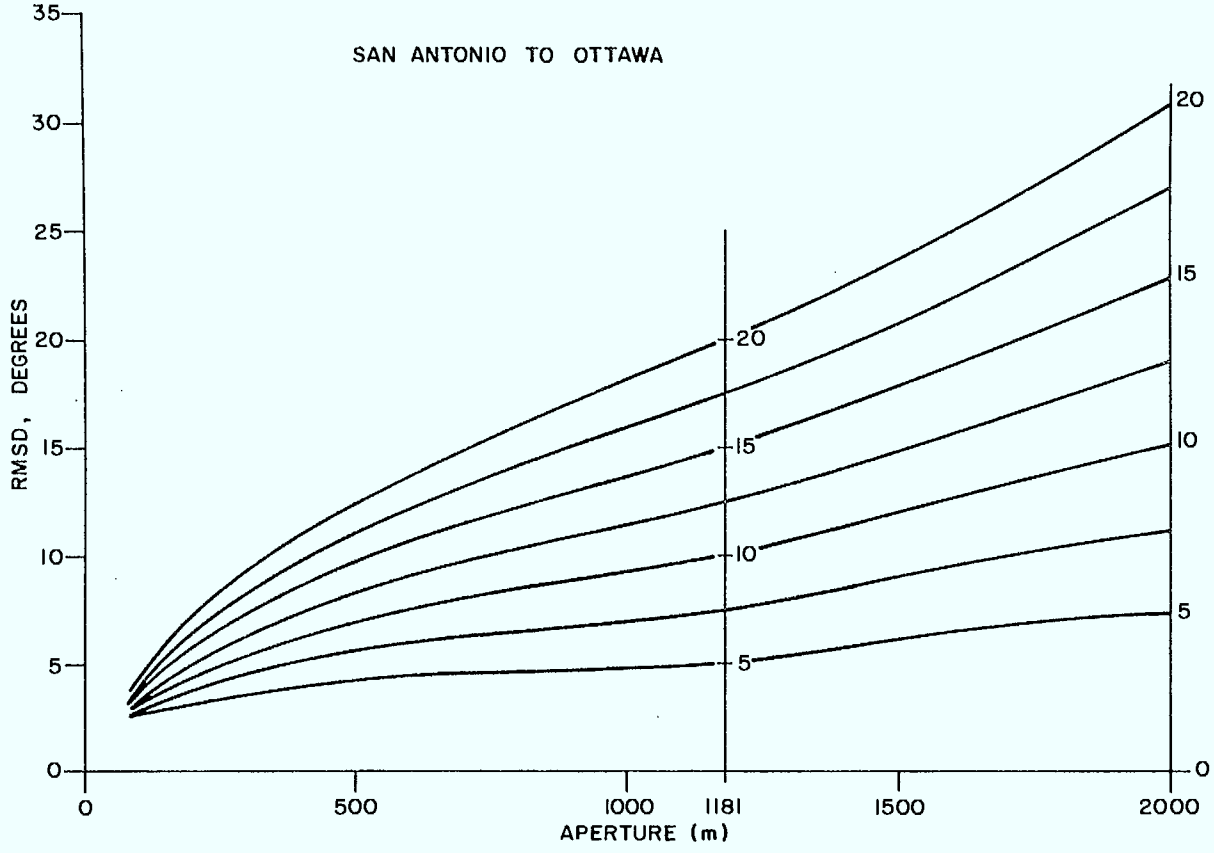

Figure 4. RMSD (with component due to residual phase errors removed) vs aperture for Test B. Curves are identified by the RMSD value at the vertical line at 1181 m.

The curves of Figure 3 and 4 represent the data from all modes, although different modes tend to contribute to different groups of curves. For example, in Figure 3 the curves for the smaller RMSD values are derived mostly from normal E-mode results, whereas the curves representing larger RMSD values are derived from 2 hop E and 2 hop E_s results. The distributions of observed RMSD for the 1181 aperture are shown in Figures 5 and 6 for each mode for Test A and Test B respectively. The points on each horizontal bar indicate values of RMSD at which the cumulative relative frequencies of occurrence are .125, .25, .375, .50, .625, .75, and .875.

The RMSD distributions for Test A for the low and high angle E mode and the E_s-2-N (cf. Table 3 for description) are very similar while that for the E_s-S-N is only slightly different, but all of them are very different from the E_s-1-N. Certain ones can be grouped, as they are very similar, e.g., 2E and $2E_s$; F2(o),L and F2(x),L; F2(o),H and F2(x),H; 2F1(o),L, 2F1(o),H and 2F1(o), near MOF. For Test B the same type of grouping can also be done.

To use Figures 3 and 5 one first scales for the mode of interest the median RMSD value from Figure 5, and then locates this value along the vertical line at 1181 m in Figure 3. The curve which would pass through

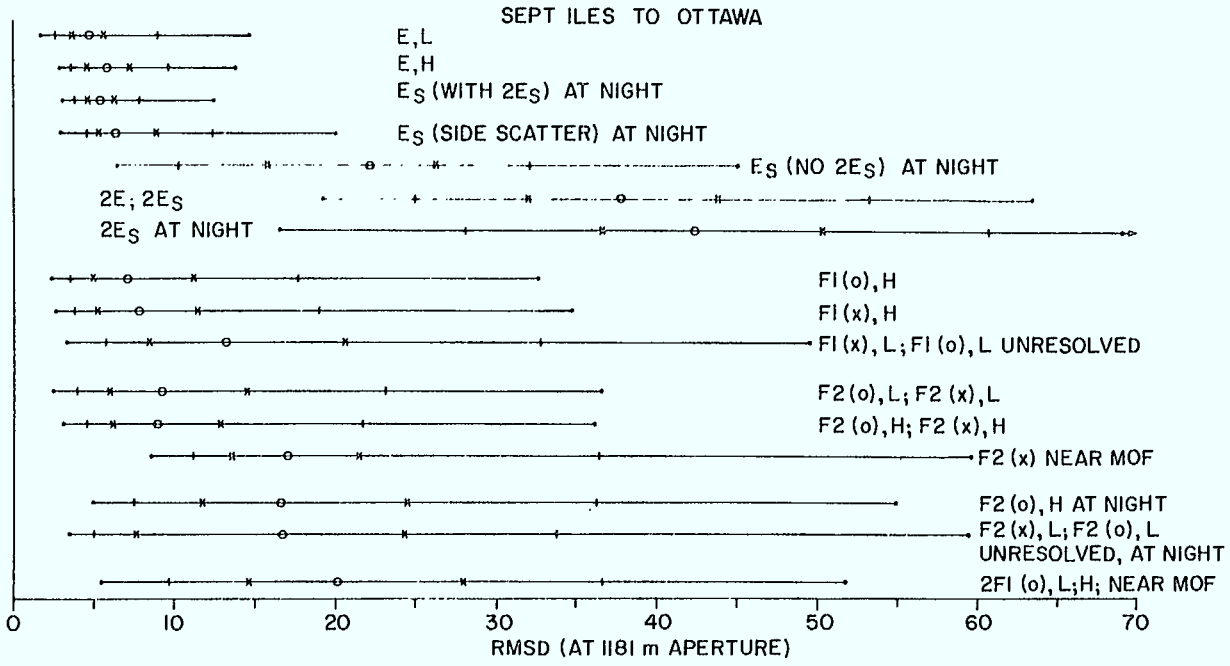

Figure 5. RMSD (with component due to residual phase errors removed) at 1181 m for Test A. The bars encompass for each mode 75% of all occurrences for that mode. Points indicate cumulative occurrence probability; legend (.) .125 and .875, (+) .25 and .75, (*) .375 and .625, (o) .50.

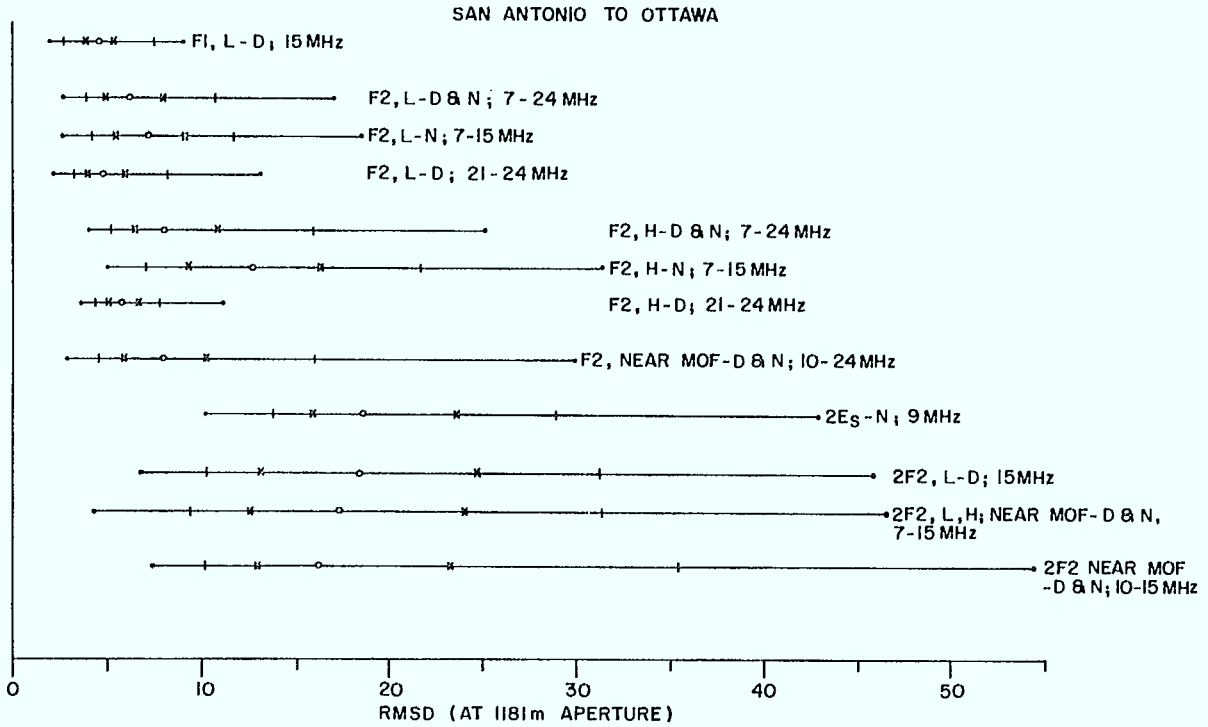

Figure 6. RMSD (with component due to residual phase errors removed) at 1181 m for Test B. The bars encompass for each mode 75% of all occurrences for that mode. Points indicate cumulative occurrence probability; legend (.) .125 and .875, (+) .25 and .75, (*) .375 and .625, (o) .50. During daytime is indicated by -D.

this value gives the variation in the median RMSD with aperture for that mode. The same applies to Figures 4 and 6.

In order to verify that not only the median could be scaled in this way, but also the other six distribution points shown in e.g., Figure 5, curves similar to those shown in Figure 3 were drawn for the seven distribution points for the low angle E mode and the combined 2E and $2E_s$ modes. Not surprisingly, the various curves matched those in Figure 3 very closely. The same was done for the low angle F2 and low angle 2F2 modes using Figures 4 and 6, with the same conclusion reached.

Distributions of the RMSD occurrence are most usefully presented as the probability that the RMSD is less than a certain threshold vs the threshold. Such a distribution for the low angle E mode for Test A is presented in Figure 7. Figure 8 illustrates the distribution for the 2E and $2E_s$ modes. In this case the RMSD was too large for meaningful residual phase errors to be obtained and so the effect they produce has not been removed from these curves. Distributions for the low angle F2 and 2F2 modes for Test B are presented in Figures 9 and 10.

3.3 CONE ANGLE (AZIMUTH) ERROR VERSUS APERTURE

Having examined the variation of RMSD with aperture, we now look at the dependence of the bearing error on aperture. The orientation of the HFDF array at Ottawa is such that the long arm is almost perpendicular to the paths from both Sept Iles to Ottawa and San Antonio to Ottawa. As a result, the azimuths of the arriving transmissions are approximately the same as the cone angles measured by the long arm. The cone angle is the angle between the axis of the arm of the array and the normal to the wavefront. Hence, cone angles are referred to as azimuths in this section. Statistics of occurrence and standard deviations of the azimuths for various apertures were tabulated for the various ionospheric modes.

The azimuths from the various time intervals for the same mode were combined to indicate the variation in the standard deviation of the azimuth as a function of aperture for each mode. Those for Test A for the various E modes are illustrated in Figure 11 and for the various F1 and F2 modes in Figure 12. It is clear that the standard deviation in the azimuth is much greater for some modes than for others. The lowest values are for the low and high angle E and the E_s-2-N, all of which, when one bears in mind the numbers of occurrences (cf. Table 3), are essentially the same.

The standard deviations of the azimuth as a function of aperture for the various modes received during Test B are shown in Figure 13. The F2,L-D results are similar to those for E,L of Test A. The standard deviation is small, and the RMSD as indicated in Figures 3 and 6 is low. The standard deviation for the F1 mode and its corresponding RMSD are small and lower than for the F2-L mode. The curves for F2,H and 2F2,L are similar and exhibit little variation with increasing aperture indicating the presence of TIDs. The 2F2 mode near the MOF has the largest standard deviation, much larger than for the F2 mode near the MOF.

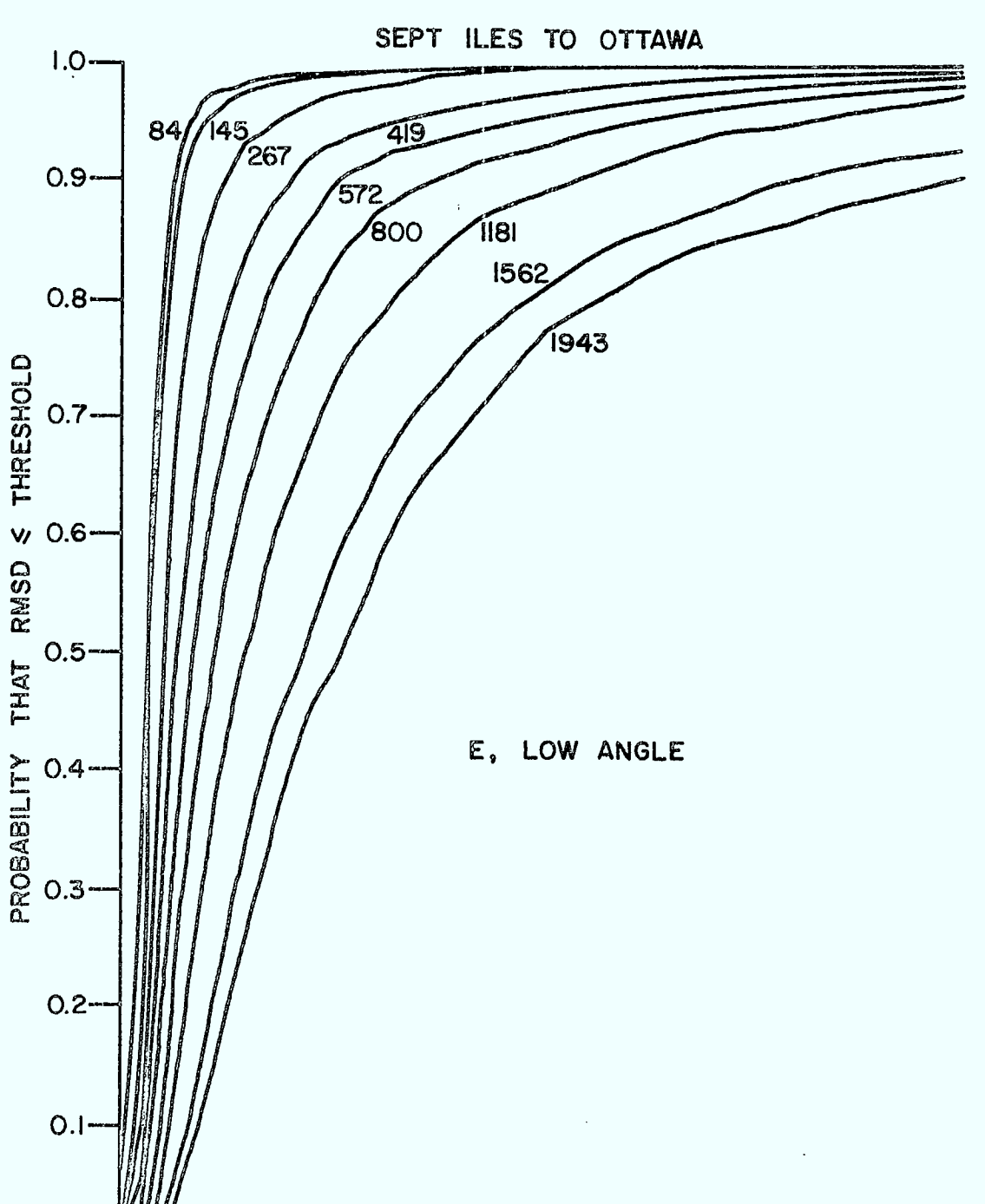

Figure 7. Probability that RMSD is ⩽ RMSD threshold vs threshold for low angle E modes on Days 171–174, 1977 for 6.8 to 7.6 MHz for Test A. Curves are labelled by aperture size in metres.

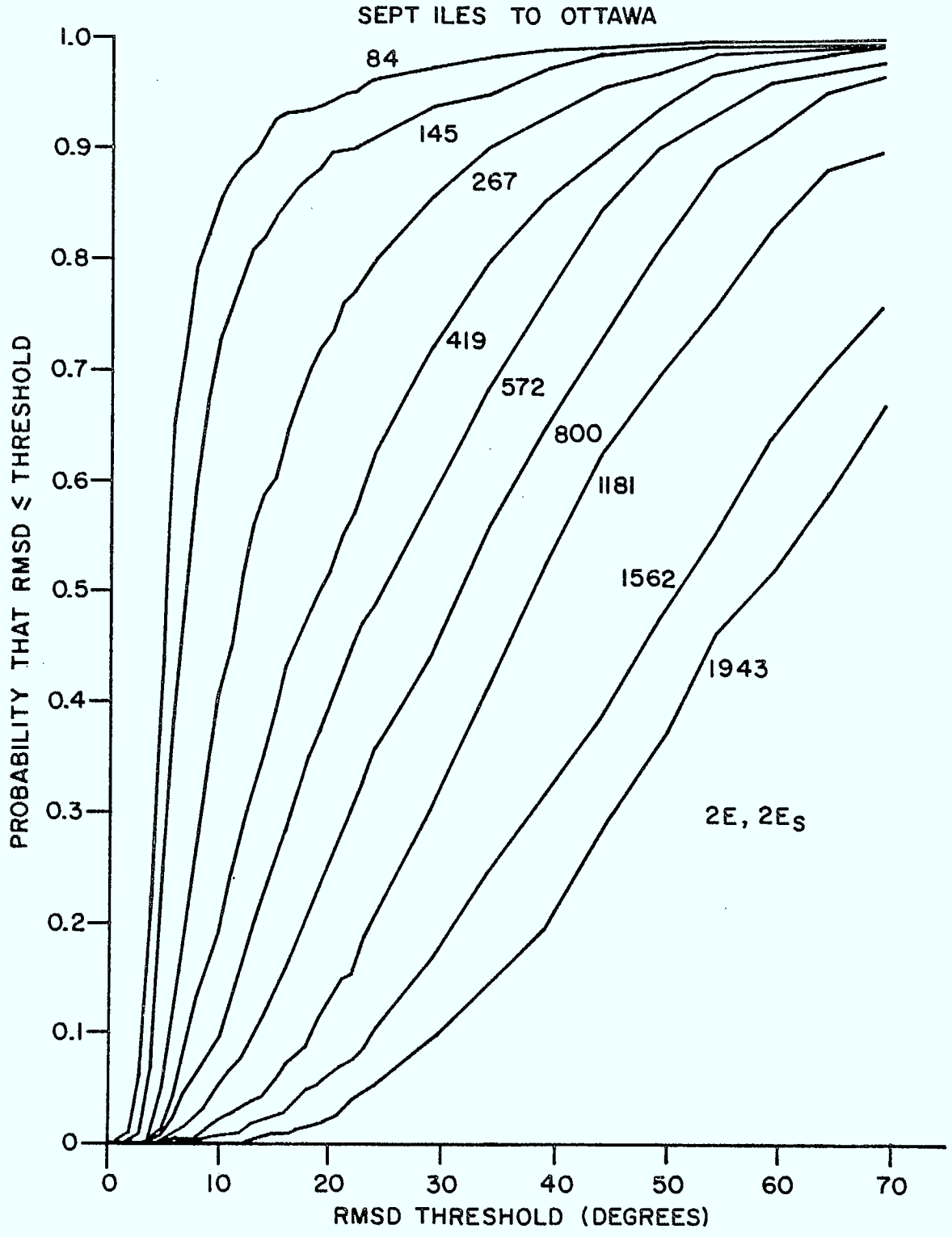

Figure 8. Probability that RMSD is ⩽ RMSD threshold vs threshold for $2E_s$ and 2E modes on Days 171–174, 1977 for 6.8 and 7.6 MHz for Test A. Curves are labelled by aperture size in metres. Residual phase error corrections were not incorporated.

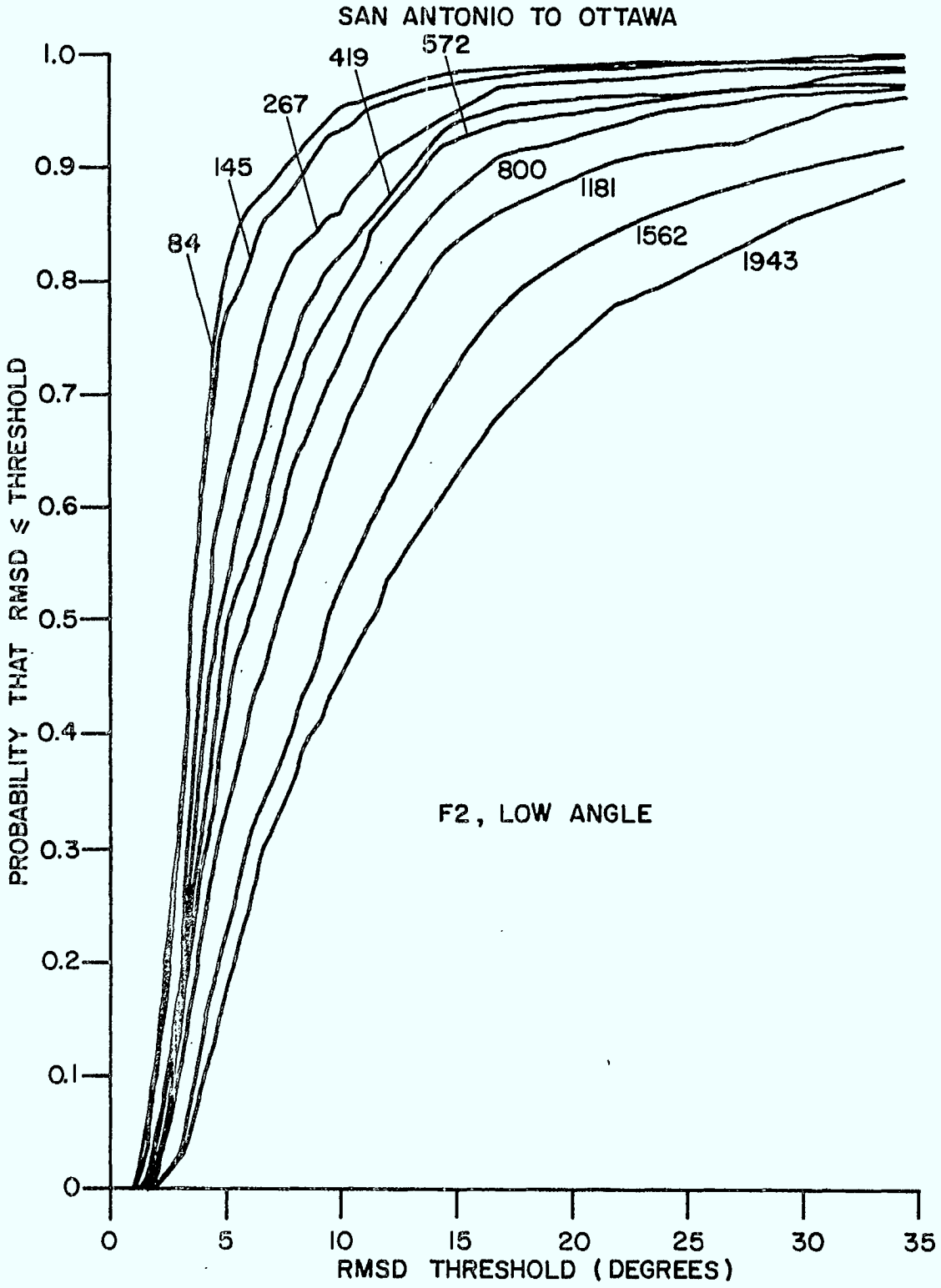

Figure 9. Probability that RMSD is ⩽ RMSD threshold vs threshold for low angle F2 mode on Days 329–331, 1977 for Test B. Curves are labelled by aperture size in metres.

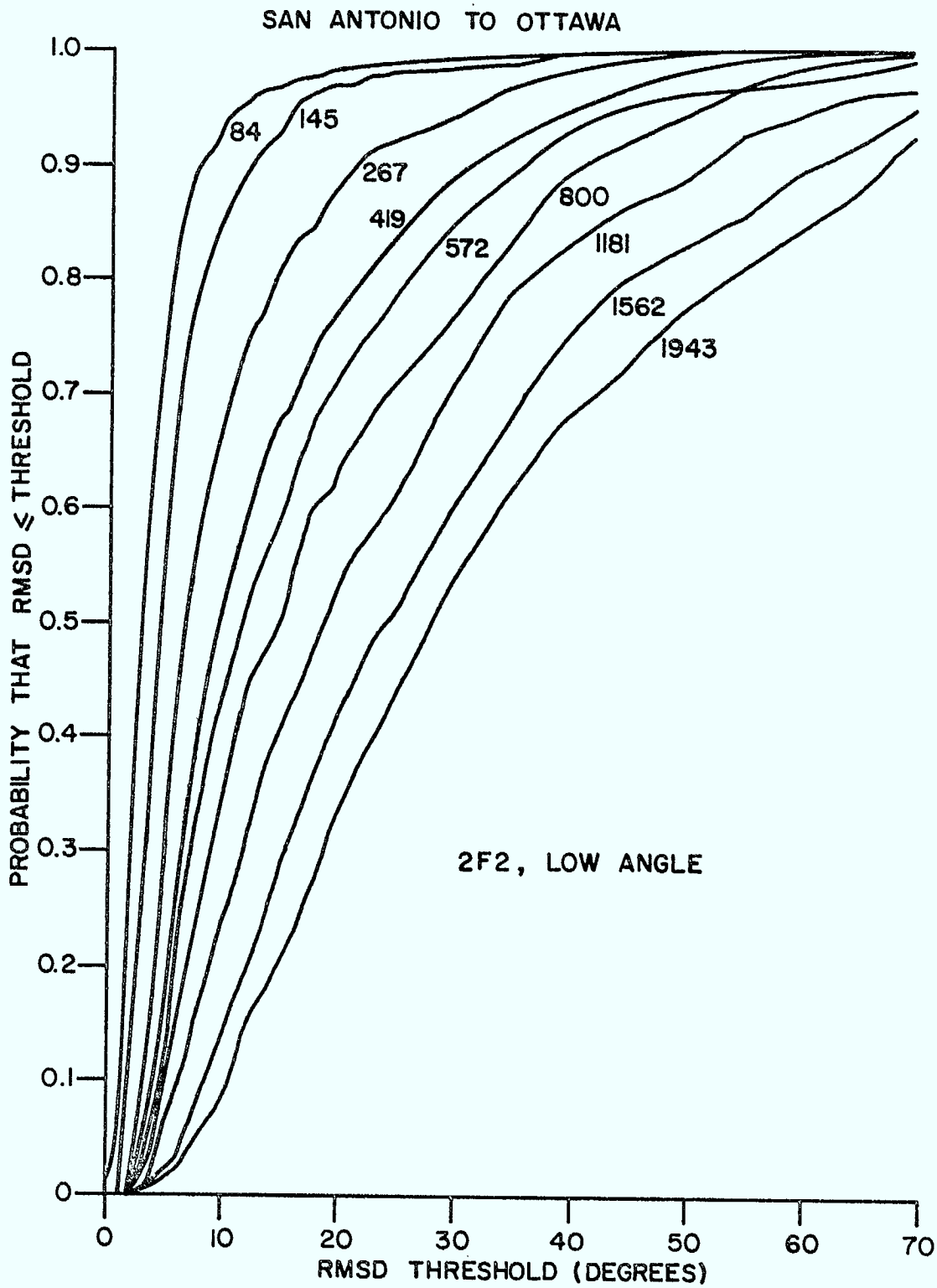

Figure 10. Probability that RMSD is ≤ RMSD threshold vs threshold for low angle 2F2 mode on Days 329–331, 1977 for 15 MHz for Test B. Curves are labelled by aperture size in metres.

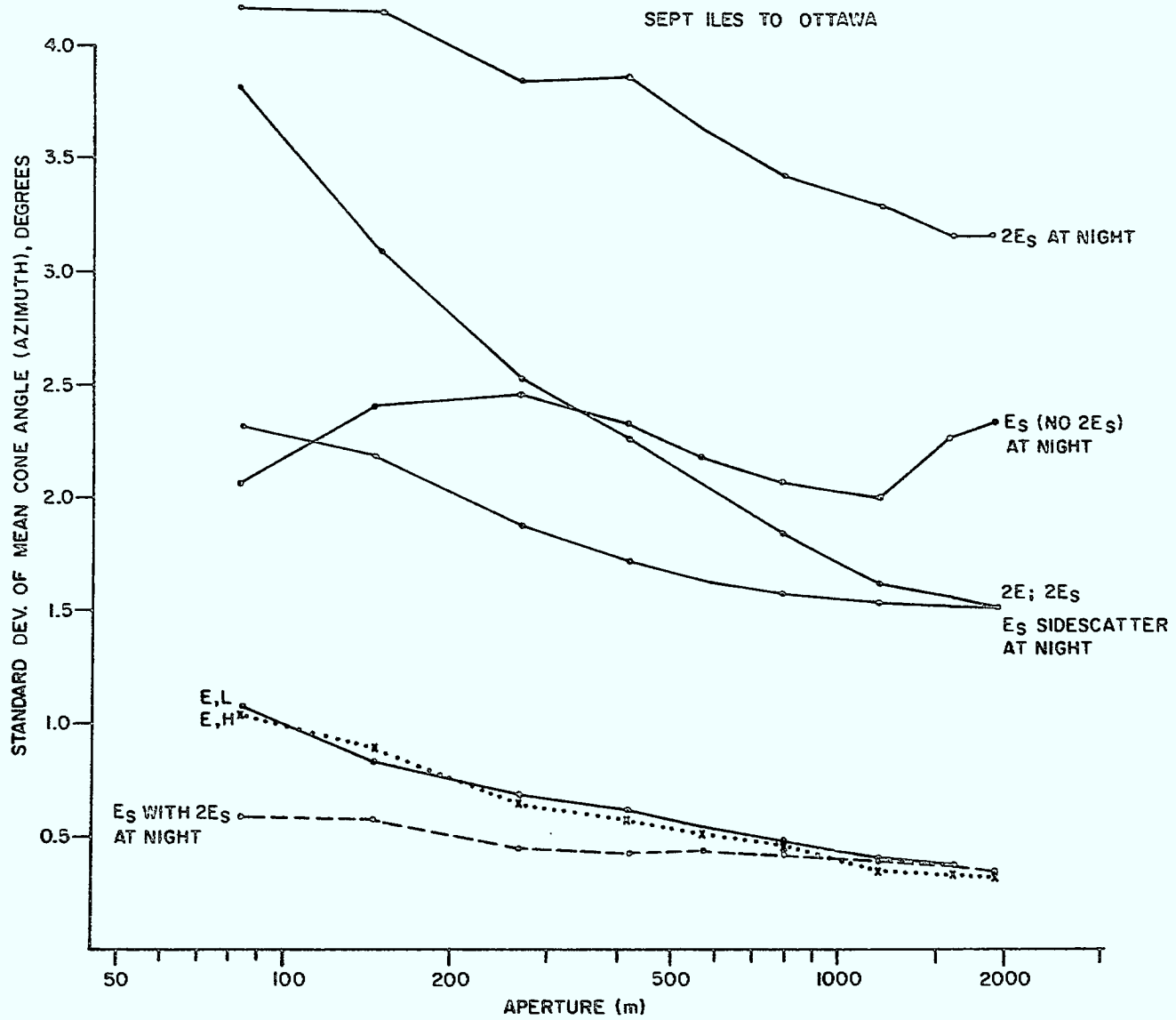

Figure 11. Standard deviation of the mean cone angle (approximate azimuth) vs aperture for various E modes for Test A.

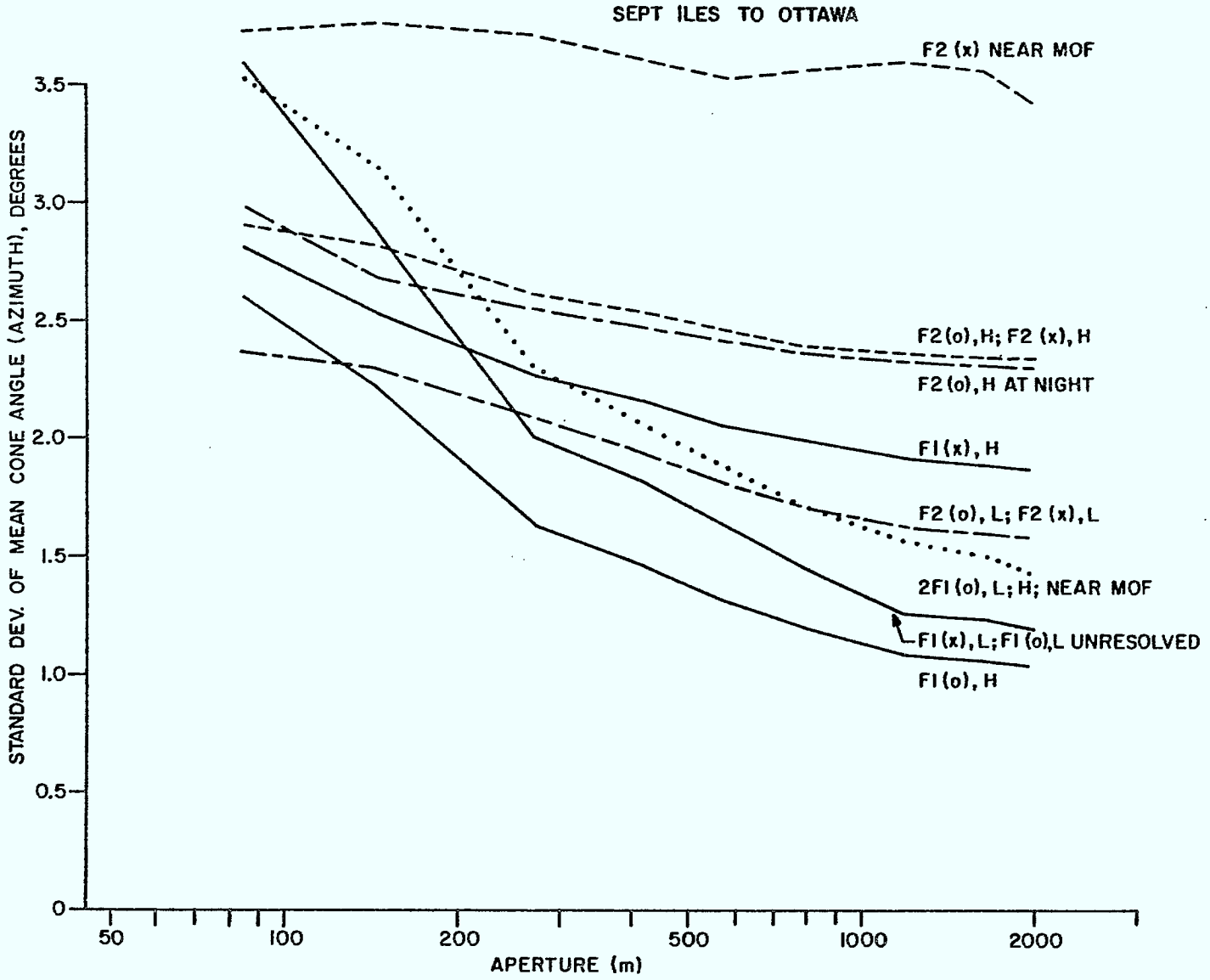

Figure 12. Standard deviation of the mean cone angle (approximate azimuth) vs aperture for various F modes for Test A.

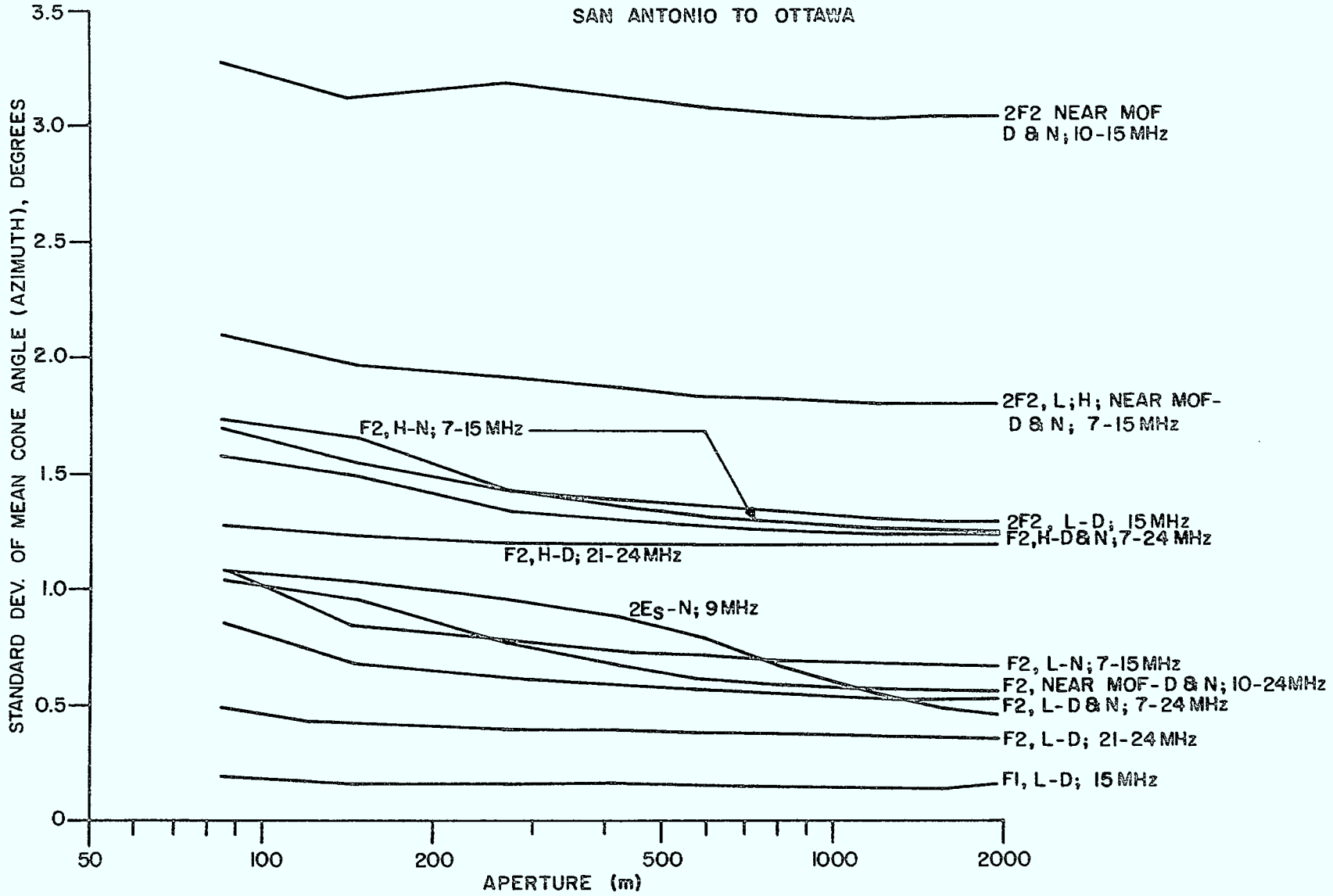

Figure 13. Standard deviation of the mean cone angle (approximate azimuth) vs aperture for various F modes for Test B. During daytime is indicated by -D.

3.4 BEARING STANDARD DEVIATION AND ERROR IN MEAN BEARING AS A FUNCTION OF RMSD THRESHOLD

In the discussion thus far, the relationships of RMSD and bearing error to aperture size have been presented. However, the first two are not independent and the relationship between these two needs exploration. In an attempt to understand the change in the azimuth error with RMSD, the occurrences of bearing were classified according to RMSD value for the largest aperture (1943 m). It was found that there was a pronounced increase in the standard deviation of the azimuth with increasing RMSD. The same is true when all bearings below a certain RMSD threshold are combined. This type of result for Test A is shown in Figure 14 where the continuous rise in the standard deviation in the azimuth with increasing RMSD threshold is clear. The same was true for Test B (not shown).

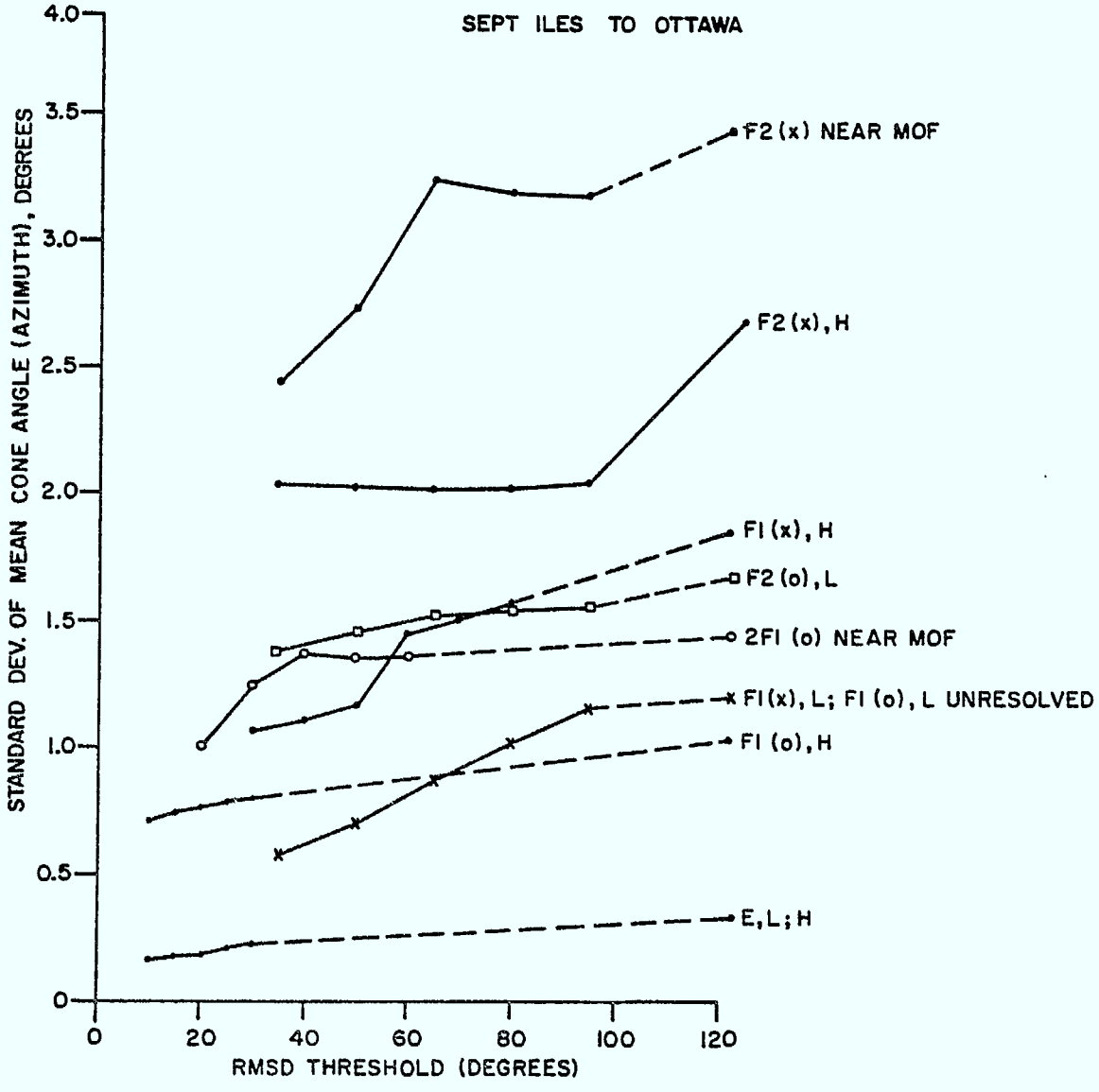

Figure 14. Results for Test A for various ionospheric modes

The estimated RMS error in the mean azimuth is the standard deviation divided by the square root of the number of statistically independent measurements. This value, as indicated by Rice (1980), when plotted as a function of RMSD threshold exhibits a minimum which is very broad. In order to check this conclusion, the results presented in Figure 14 for Test A and the result for Test B were converted to values of RMS error in the mean azimuth, assuming statistically independent samples. The results for representative modes are presented in Figures 15 and 16 for Tests A and B respectively. The number of occurrences at certain thresholds is indicated, to give a more complete presentation. As can be seen, the minima are indeed broad, indicating that the precise choice of an RMSD threshold is not important since the RMS error in the mean azimuth changes negligibly as the threshold is changed. The optimum threshold value, broad as it is, may be mode dependent, and for Test A may be near 20 degrees for the E mode and 80 degrees for the low angle F2(o) mode and high angle F2(x) mode. For Test B the optimum threshold value may be near 20 degrees for F2,L and near 50 degrees for the F2,H and 2F2 modes.

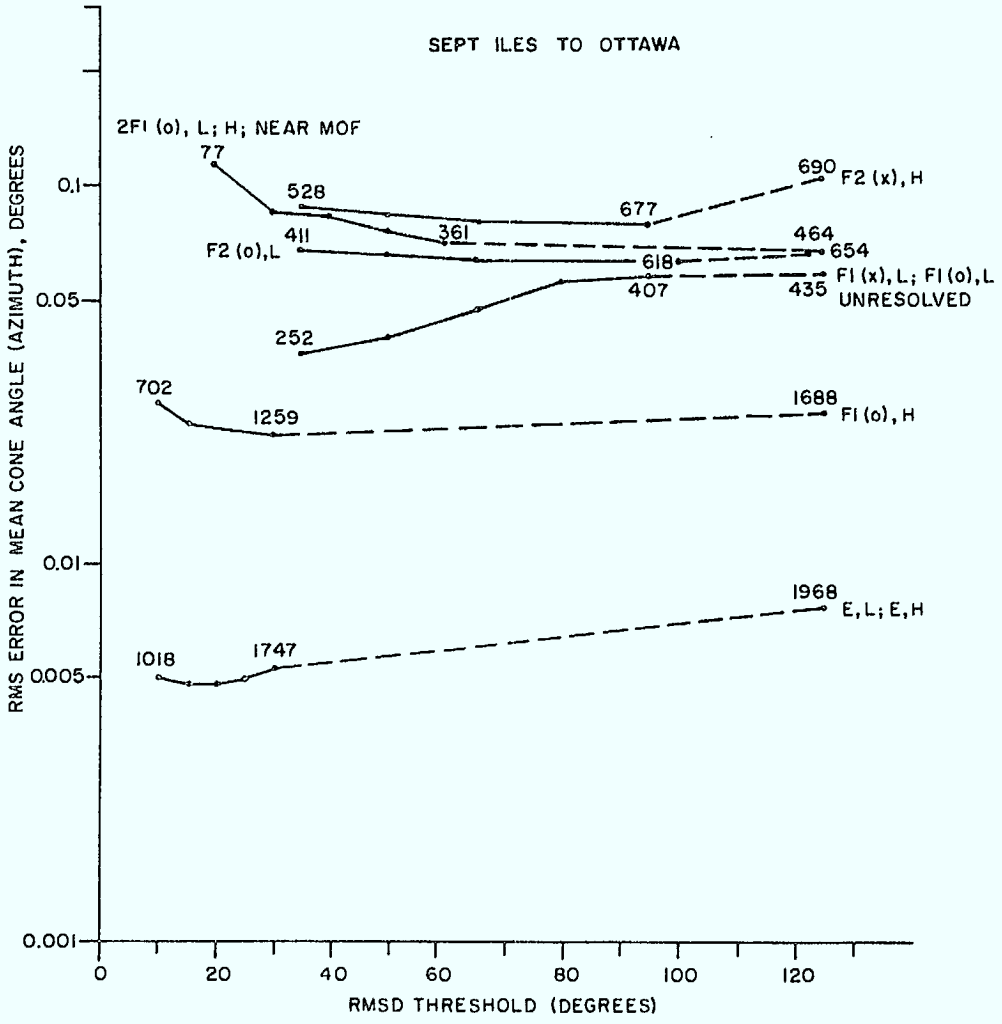

Figure 15. Results for Test A for various ionospheric modes

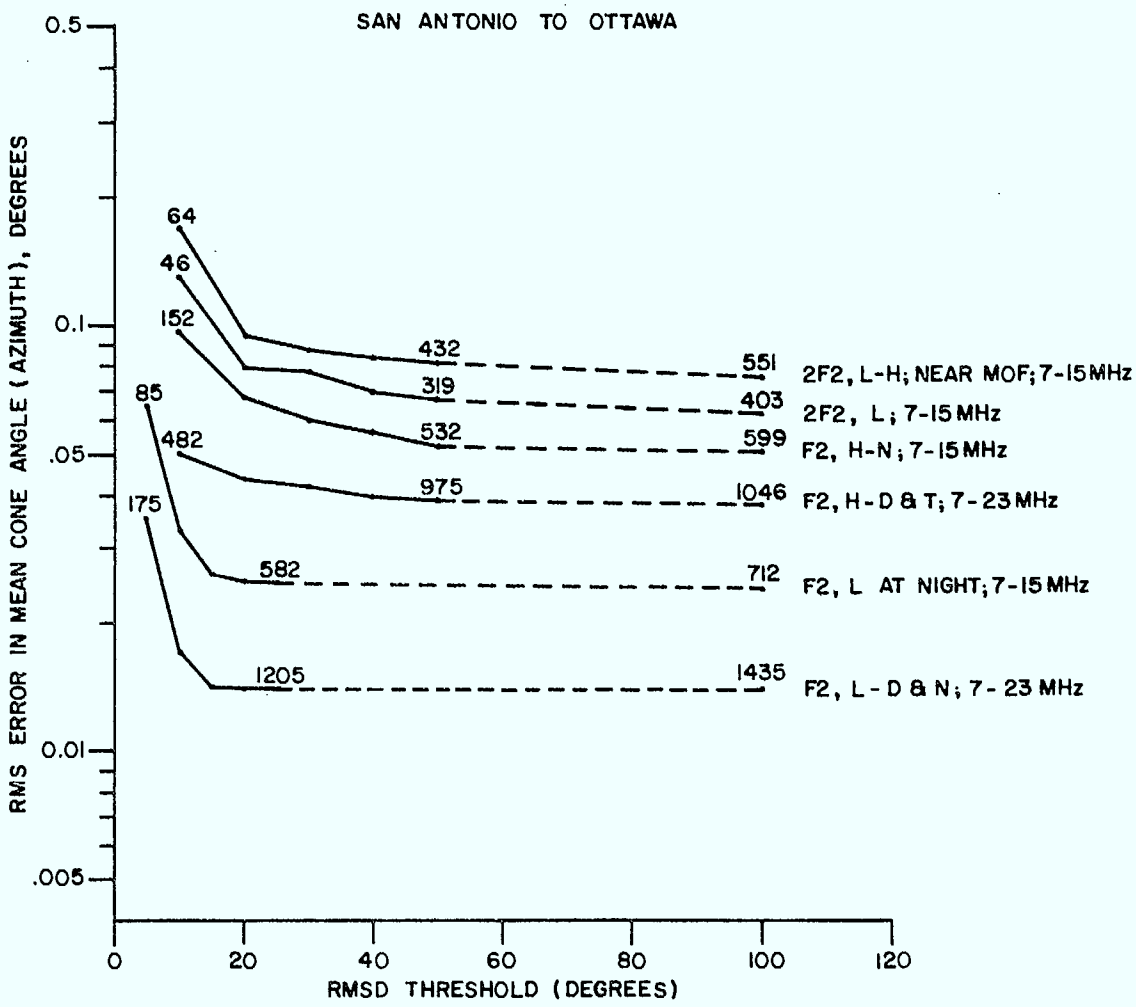

Figure 16. Results for Test B for various ionospheric modes. During daytime is indicated by -D.

4. DISCUSSION AND CONCLUSIONS

An FMCW sounding experiment was carried out between (a) Sept Iles and Ottawa (a 911 km path), in June 1977, and (b) San Antonio, Texas and Ottawa (a 2654 km path) in November 1977, to examine the relationship between DF accuracy, wavefront planarity and aperture size. For the test the long arm of an 1181 m by 236 m crossed linear array at the SARA site was extended northward to 1943 m. Over the medium length midlatitude path transmissions via E, 2E, F1, F2 and 2F1, broken down into different modes and components, were examined; and over the long midlatitude path F1, F2, 2F2 and $2E_s$ modes were studied. The data for the 1943 m arm were processed in sub-sets so as to provide results for 9 different aperture sizes.

The measure of wavefront planarity used was the RMS of phase deviations from a straight line fit to the phase front, and such deviations, weighted by the normalized mean space between adjacent antennas, yielded values of RMSD. For each test, the RMSD distribution and RMSD as a function of aperture was

presented for all modes by a graph of median RMSD vs aperture on which were drawn a series of curves of wavefront roughness or nonlinearity (identified by the value of the RMSD at the 1181 m aperture). These curves can be used to either predict for the two test paths used, or estimate for test paths between them, the RMSD for any aperture up to 2000 m knowing the RMSD for any other aperture. Companion graphs for the two test paths illustrate for the various ionospheric modes possible, seven points on the RMSD distribution curve for the 1181 m aperture. Those curves permit the estimation of the RMSD value for any aperture for these modes. The pairs of figures are Figures 3 and 5 and Figures 4 and 6.

It was also found that if one is to conduct wavefront tests using an aperture less than 200 m, they should realize that uncertainties in the wavefront due to residual errors in receiver phases (site and system errors) could become as important as multipath and multimode corrugations in the wavefront.

Two important points were revealed by Figures 5 and 11. In Figure 5, for the medium path test, the RMSD distributions are similar for the E_s (with $2E_s$) at night and E_s (sidescatter) at night, whereas, as indicated in Figure 11, the standard deviation in the cone angle for the E_s (with $2E_s$) at night is much smaller. This meant that (i) although the RMSD is a measure of wavefront planarity and the RMSD occurrence distribution reveals details of the presence and magnitude of corrugations in the wavefront, the RMSD may not necessarily reveal details about azimuthal accuracy. (ii) The standard deviation in the cone angle (azimuth), which indicates a shifting about of the apparent azimuthal angle of arrival, may not necessarily be related to the RMSD (planarity of the wavefront).

The RMSD distribution curve in Figures 7 and 8 for the medium path test may be compared to those of Rice (1975). His curves are very similar, and differ from these in the same way as those from any one test period differed from them. The experimental curves presented here for the smaller apertures are typical of the results which are obtained when the aperture is small compared with the spatial period of the wave interference pattern.

A breakdown of the cone angle (azimuth) results for the 1943 m aperture as a function of RMSD reveals, for both tests concerned, an increase in the standard deviation of the azimuth with increasing RMSD threshold. When the standard deviation is converted to RMS error in the mean azimuth (standard deviation divided by square root of occurrences) the same type of broad minimum was found as reported by Rice (1980), indicating that the precise choice of an RMSD threshold is not important.

The variation in the standard deviation of the azimuth as a function of an aperture for each mode for the two test periods was presented for a variety of modes. Some of the curves exhibited considerable variation with aperture e.g., 2E and $2E_s$, F1(o,x),L and the combined 2F1(o),L,H and near MOF. This is presumably because there is more multi-path wave interference within those modes, an interpretation consistent with the RMSD distributions shown in Figure 5. Other curves exhibit a flatter variation e.g., E_s-S-N, combined F2(x),H and F2(o),H. This is probably due to reflections from TIDs or reflections from irregularities similar to them. At such times, two or more paths for the same mode are probably present with the wavefront from

each path being fairly planar. Since only one raypath was chosen from each minute of data (the raypath with the strongest signal) an apparent switching about in the azimuth can appear in the results. Such a switching about was occasionally unambiguously identifiable in the data. The result can have a fairly large standard deviation in the bearing, and a value which is about the same for all aperture sizes. This interpretation is consistent with the RMSD distribution shown in Figure 5. In the case of F2(x),H and F2(o),H the effects of TIDs were identifiable in the data. In the case of F2(x) near the MOF, the results are not clear as they represent many isolated periods when bearings were radically different. Based on the various plots for the San Antonio to Ottawa path (Test B), the F1 is rarely received over such a long path (2654 km) and the F2 high angle is the dominate mode. Because this mode is significantly influenced by ionospheric tilts, the RMSD can be low, yet the corresponding standard deviation of the bearing is high.

It is also possible to speculate about the number and relative power of rays received via the various modes. Based on the theoretical work of Rice (1980), the RMSD distribution for the E and E_s-2-N modes of Test A suggest that the wavefront for apertures less than 1943 m could be due to signals from two ray paths, the power of the first dominating by a factor of 16. In the case of the F1 and F2 modes the same appears to hold but the factor could be near nine. This same speculation can be carried out on the results of Test B. For this test the F1 and F2 modes have the lowest RMSD and this suggests that one raypath dominates the transmission of these modes. In the case of the two hop modes the high RMSD suggests that two ray paths of nearly equal signal power may be responsible.

The various figures presented in this report which are based on test over 900 and 2500 km paths can be helpful in DF design when used in conjunction with economic and physical considerations. Figures 5 and 6 can be used to identify the modes to be expected, and these figures, in conjunction with Figures 3 and 4 the wavefront planarity for the aperture of interest. Figures 11 to 13 can be used to indicate the degree of accuracy to which the bearing could be measured for the aperture of interest.

5. ACKNOWLEDGEMENTS

The author is indebted to Drs. D.W. Rice and G. Atkinson for fruitful discussions and comments. This work was supported by the Department of National Defence of Canada.

6. REFERENCES

Burke, M., *Calibration of the C.R.C. High-Frequency Direction-Finding Receiver Systems at Ottawa*, CRC Technical Note 690, 1978.

Montbriand, E., *Residual Phase Errors in the CRC HF Sampling Array*, CRC Technical Note in preparation.

Rice, D.W., *Phase Characteristics of Ionospherically Propagated Radio Waves*, Nature Physical Science, 244, #136, 86, 1973.

Rice, D.W., *High Resolution Measurements of Time Delay and Angle of Arrival Over a 911 km HF Path*, AGARD Conference Proceedings on Radio Systems and Its Ionosphere, Paper 33-1, 1975.

Rice, D.W., *HF Direction Finding by Wavefront Testing*, CRC Report 1333, 1980.

Rice, D.W. and Winacott, *A Sampling Array for H.F. Direction-Finding Research*, CRC Report 1310, 1977.

MONTBRIAND, L.E.
--The dependence of HF direction
finding accuracy on aperture size.